



RICE UNIVERSITY

DETERMINATION OF VAPOR-LIQUID EQUILIBRIA
BY HORIZONTAL BUBBLE COLUMN CHROMATOGRAPHY

by

Charles J. Perilloux

A THESIS SUBMITTED
IN PARTIAL FULFILLMENT OF THE
REQUIREMENTS FOR THE DEGREE OF

MASTER OF SCIENCE IN CHEMICAL ENGINEERING

Thesis Director's Signature

H. A. Deans

Houston, Texas

June, 1968

ABSTRACT

DETERMINATION OF VAPOR-LIQUID EQUILIBRIA BY HORIZONTAL BUBBLE COLUMN CHROMATOGRAPHY

Charles J. Perilloux

When a series of closely spaced gas bubbles flows with the surrounding liquid in a small tube, the gas velocity will be greater than that of the liquid due to the thin stationary liquid film along the tube walls. This velocity separation meets a prime requirement for a chromatographic system.

If a pulse of radioactive tracers is injected into such a system, the retention time of each tracer component will depend only on the gas and the liquid velocities, the relative amounts of liquid and vapor in the column, and the vapor-liquid equilibrium K value of the component. Thus, a bubble column can be used to determine K values.

This work determined the K value of ethane at 74 °F and one atmosphere at infinite dilution in the helium-*n*-decane system to be 26.6 ± 2.1 . This compares favorably with data taken by static means.

The peak dispersion coefficient increased with the square of the bubble velocity. The film thickness vs. velocity agreed well with theory.

The method has been extended in theory to the general case of n components with each component present in both phases.

ACKNOWLEDGMENTS

The author wishes to express his appreciation to the following for their assistance in this work:

Dr. H.A. Deans -- for his guidance and counsel throughout this work as thesis advisor,

Dr. J.W. Hightower -- for his suggestions and aid in radioactive tracer techniques,

Dr. Riki Kobayashi -- for his suggestions concerning extension of experimental technique,

Mr. J.B. Galeski -- for his assistance in transferring the tracer samples,

Rice University and the National Science Foundation -- for the financial support of the author and the research work, respectively, and

The author's wife, Kathy -- for her patience and encouragement throughout his graduate studies.

TABLE OF CONTENTS

	Page
Title Page	i
Acknowledgments	ii
Table of Contents	iii
Table of Nomenclature	iv
I. INTRODUCTION	1
II. DESCRIPTION OF EXPERIMENTAL APPARATUS	5
III. EXPERIMENTAL PROCEDURE	14
IV. THEORY	18
V. EXPERIMENTAL RESULTS	23
VI. DISCUSSION OF RESULTS	29
VII. CONCLUSIONS AND PROJECTION OF TECHNIQUE	33
Appendix A. Calculations	34
Appendix B. Discussion of Isotope Effects	40
Appendix C. Extension of Techniques	42
Appendix D. Original Data	45
Bibliography	46

TABLE OF NOMENCLATURE

A_G	area open to gas flow, cm^2
A_L	area open to liquid flow, cm^2
A_T	average cross-sectional area of tube, cm^2
b	average film thickness, cm
B	peak width at half height, sec
\bar{B}	normalized peak width, dimensionless ($\equiv BV_L/L'$)
B^*	peak width, cm ($\equiv \bar{B} L'$)
C_L	quantity of liquid per unit column length, moles/cm
C_V	quantity of vapor per unit column length, moles/cm
D_0	overall dispersion coefficient, cm^2/sec
F	bubble frequency, sec^{-1}
F_L	volumetric liquid flow rate, cm^3/sec
K_i	vapor-liquid equilibrium constant ($\equiv y_i/x_i$)
L	molar liquid flow rate, moles/sec
L'	column length, cm
L_B	effective bubble length, cm
L_L	effective fillet length, cm
M_A	average liquid molecular weight, g/mol
M_i	molecular weight of component i , g/mol
P_{av}	average column pressure, atm
Q	weight of liquid sample collected in time θ , g
r	tube radius, cm
R	gas law constant
R_i	rate of transfer of component i from one phase to another, moles/sec

TABLE OF NOMENCLATURE (Cont.)

s	relative separation, dimensionless ($\equiv (V_G - V_L)/V_L$)
T	temperature, °R
V	molar vapor flow rate, moles/sec
V_G	gas velocity, cm/sec
V_L	average liquid velocity, cm/sec
V_i	characteristic velocity of component i, cm/sec
v_L	volume of liquid per unit bubble, cm^3
v_G	volume of gas per unit bubble, cm^3
x_i	mole fraction of i in the liquid phase
y_i	mole fraction of i in the gas phase
z_i	overall mole fraction of i in a two phase mixture
z_i^*	overall mole fraction of i in the two phase column feed mixture
z	parameter in equation of state, $PV = zRT$
α_i	$1/K_i$
θ	liquid sample collection time, sec
μ	liquid viscosity, poise
ρ_L	liquid density, g/cm^3
σ	surface tension, dynes/cm

I INTRODUCTION

The purpose of this work was to demonstrate the feasibility of using a horizontal bubble column chromatograph for the determination of vapor-liquid equilibrium K values.

An essential feature of gas-liquid chromatographic systems is the existence of a difference in velocity between the liquid and vapor phases. Standard gas-liquid partition chromatography meets this requirement with a flowing continuous vapor phase and a fixed discontinuous liquid phase adsorbed on a stationary solid support.

Numerous investigators have used standard packed column chromatographs for the determination of vapor-liquid equilibria and have obtained results consistent with data taken by static means. Stalkup and Kobayashi¹² determined the equilibrium K values of ethane and other light paraffins at infinite dilution in n-decane using methane as a carrier gas. Their work covered a wide range of temperature and pressure.

Vertical bubble columns, as investigated by Owen⁹ and Rambin¹⁰, have an essentially stationary liquid phase in which vapor bubbles rise due to their buoyancy. Owen used tritiated ethane (for radioactive detection) to determine the K value of ethane at infinite dilution in the helium-n-decane system. Rambin studied the longitudinal dispersion in the liquid phase of a vertical bubble column to determine the conditions under which dispersion would be minimized. This type of column

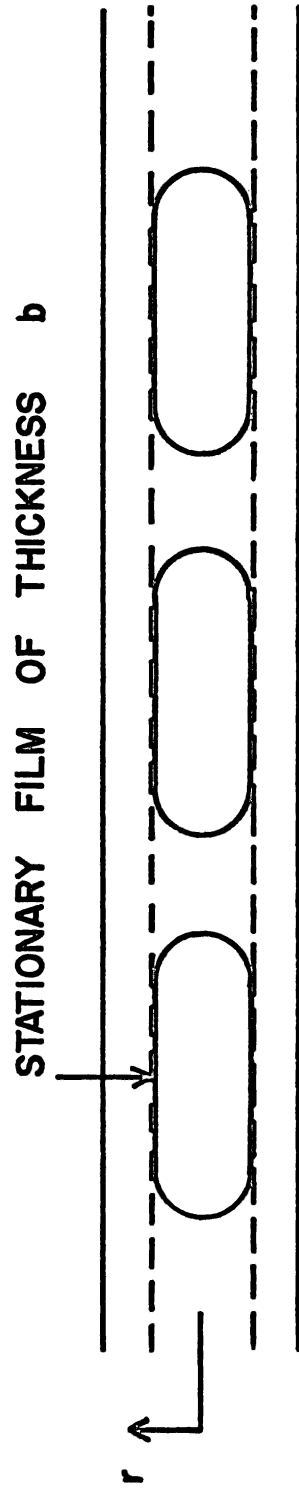
is somewhat inflexible, however, since the column radius is critical and must be changed for every new combination of flow rate and component physical properties.

In a horizontal bubble column chromatograph, both phases are flowing, but at different velocities. The bubble column chromatograph employed in this work consists of horizontal tubing containing a succession of closely spaced gas bubbles flowing through a liquid phase. The liquid fillets between the gas bubbles move at the same velocity as the gas, but the liquid film between the bubble and the tube wall is nearly stationary. Thus, the average liquid velocity is less than that of the gas and the essential requirement of gas-liquid chromatography is met. The hydrodynamic theory for both horizontal and vertical bubble flow has been developed by Bretherton².

If a sample of various components is injected as a pulse into such a bubble column, the characteristic velocities of each component will depend only on the velocities of the vapor and the liquid phases; the relative amounts of vapor and liquid in the column; and the vapor-liquid equilibrium K value of each component. Therefore, as Deans⁴ has shown, such a column could be used to determine the K value of each component.

Measurement of the characteristic velocities can be easily accomplished using radioactively tagged tracers for the injection sample. For accurate interpretation of the data, however, it is important that dispersion or peak spreading be held to a minimum. Claypool³

investigated the horizontal bubble column to determine the conditions for minimum dispersion. Gas phase dispersion in a bubble column should be negligible due to the discontinuous nature of the phase, so his research was centered on reducing liquid dispersion. His results indicated that overall dispersion could be held to a reasonable level, a necessary preliminary to this work.



SEQUENCE OF BUBBLES AND LIQUID FILLETS
FLOWING IN A HORIZONTAL TUBE

FIG. 1

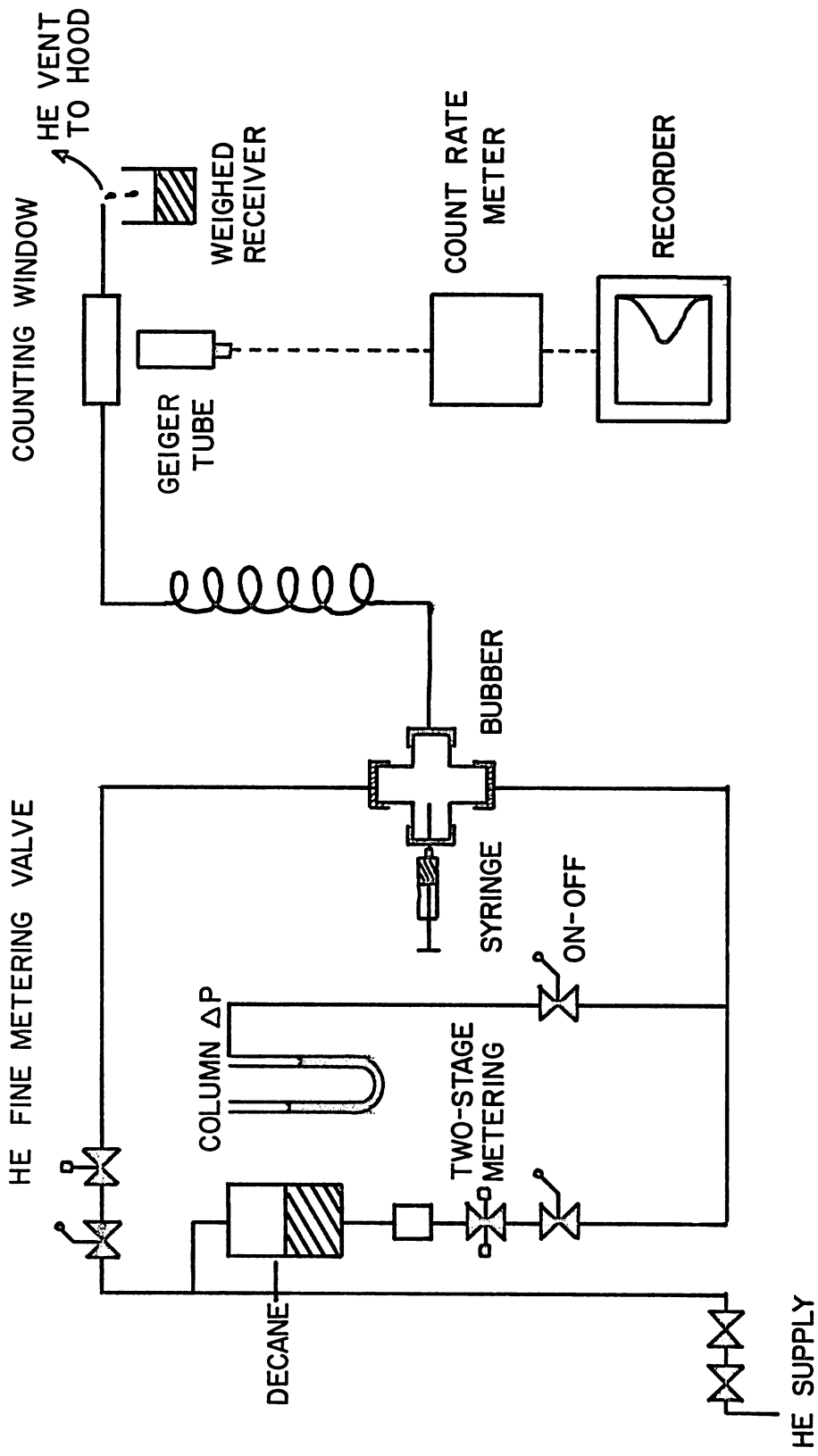
II DESCRIPTION OF EXPERIMENTAL APPARATUS

A diagram of the experimental apparatus is shown in Figure 2.

The gas used was oil-free helium, which was also used to pressurize the liquid phase. The pressure was reduced from cylinder pressure to about 50 psig by a Matheson regulator on the cylinder. Column pressure was maintained constant in the 0.1 to 0.7 psig range with a Kendall air pressure regulator. A Nupro Series S fine metering valve controlled the helium flow to the column.

The liquid phase was n-decane (99% mol pure, obtained from Matheson and Coleman) and was chosen because of its low volatility. In addition, its membership in the paraffin series would provide more nearly ideal solution with methane and ethane. The decane was fed from an aluminum cylinder pressurized by the helium. A Nupro two micron filter was placed ahead of a Nupro series M metering valve which controlled the liquid flow rate.

The bubbling device shown in Figure 3 was a cross of 2mm I.D. x 7mm O.D. Pyrex tubing. The gas phase entered through the upper arm and the decane entered through the lower arm. The two phases flowed together into the right member in which there was a slight constriction. The smaller cross-sectional area prevented liquid flow until a sufficient amount of liquid had accumulated, which then passed all at once through the constriction. This produced a steady flow of uniform bubbles separated by thin fillets of decane.



COLUMN & DETECTION SYSTEM

BUBBLER DEVICE

FEED SYSTEM

FIG. 2

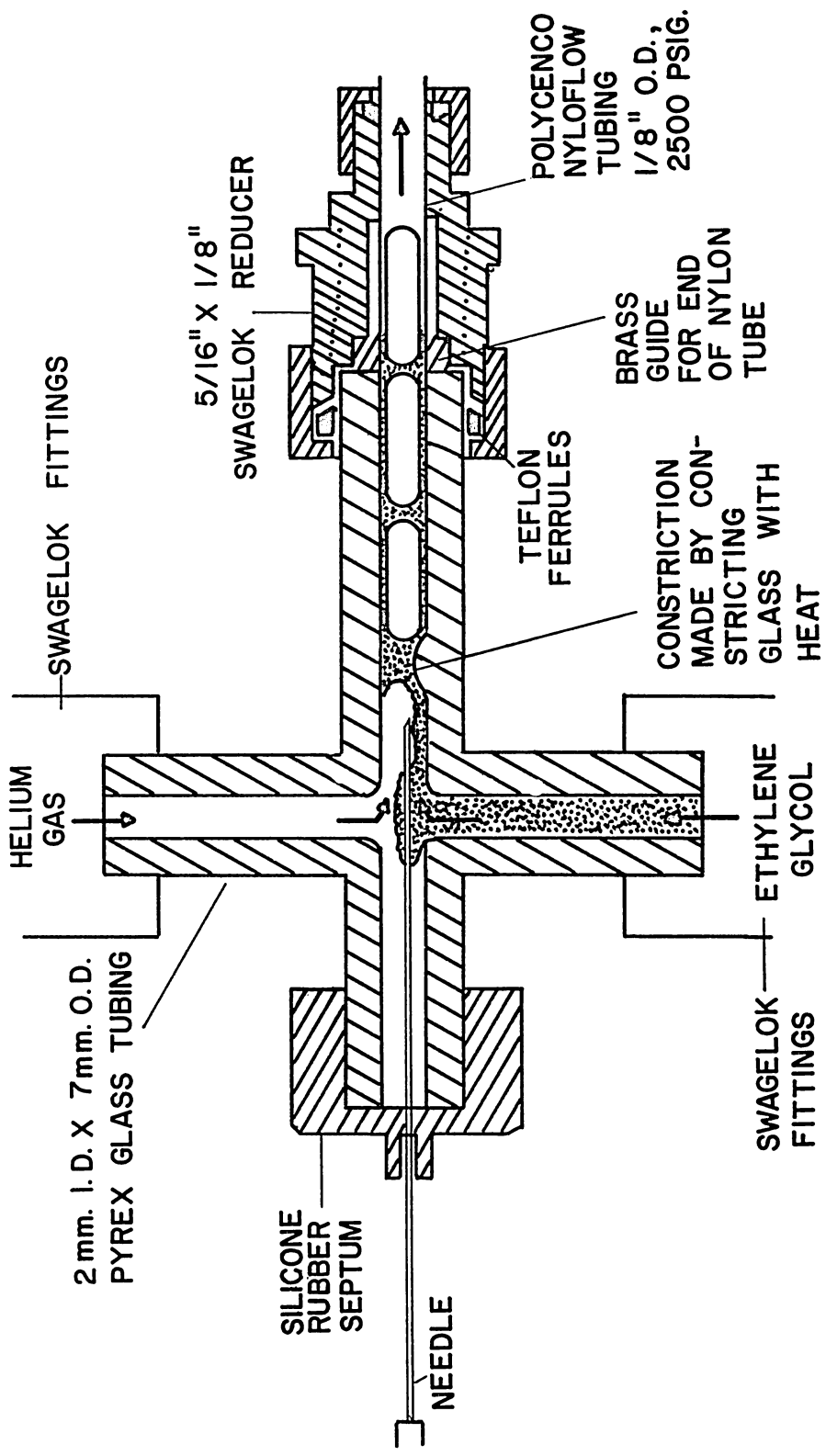


DIAGRAM OF BUBBLE DEVICE

FIG. 3

The left member of the cross served as the sample injection port. A rubber cap was fitted over the end of the tube arm. A Hamilton .05 ml gas-tight syringe was inserted through the rubber cap to inject carbon-14 methane, ethane and decane simultaneously.

The bubbler was connected by Swagelok fittings with nylon ferrules to one of the main columns, a 10.38 or a 22.78 meter length of 1/8" Polypenco nylon tubing with a volumetrically measured cross-sectional area of $.0288 \text{ cm}^2$. The tubing was coiled in several large loops (about two feet in diameter) in order to fit the whole assembly under the ventilator hood.

At the end of the tubing was the radiation detection device as shown in Figure 4. This was a small 3 x 3 inch piece of Plexiglas, drilled and tapped for fittings and with a semicircular groove cut into its surface. This groove was of the same size as the column tubing to prevent collapse of the fillets. A very thin piece of lightweight household aluminum foil was bonded with Shell Epon resin to the Plexiglas block. This very thin window was necessary due to the very low energy and penetrating power of carbon-14 beta rays.

Immediately above the foil window was suspended a thin window (1.4 mg/cm^2) Geiger-Muller tube connected to a Nuclear-Chicago model 1620A count rate meter. The meter output was fed to a variable speed, variable range Honeywell strip chart recorder.

The carbon-14 methane and ethane received from Nuclear-Chicago

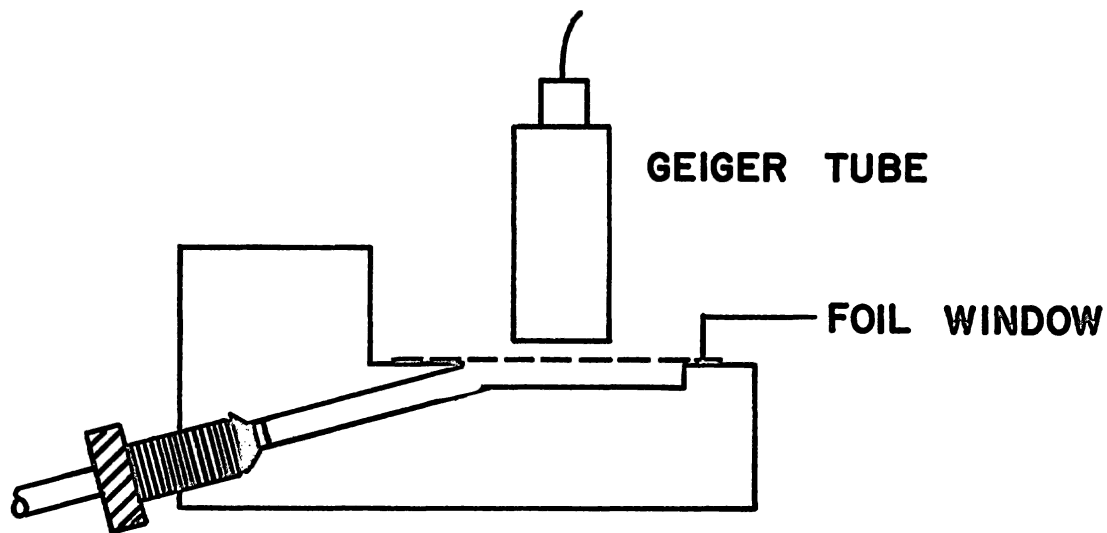
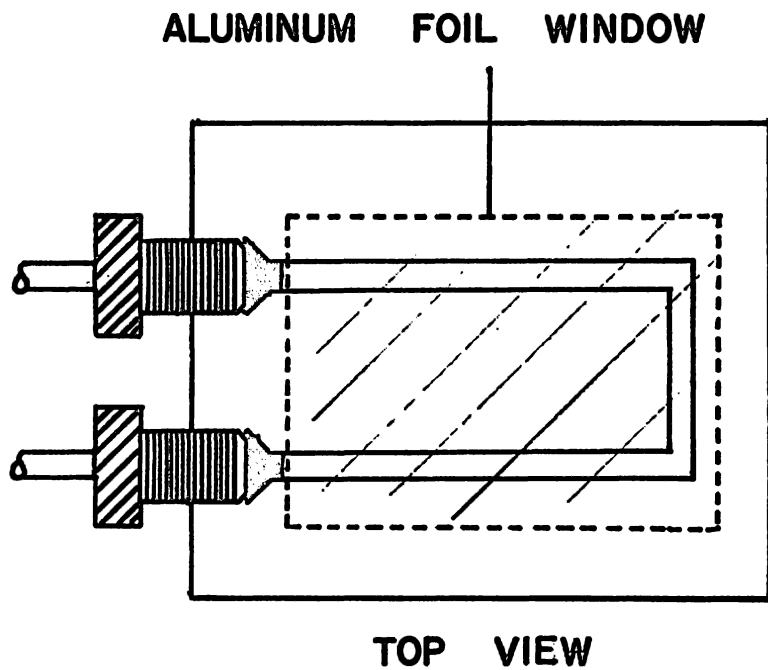


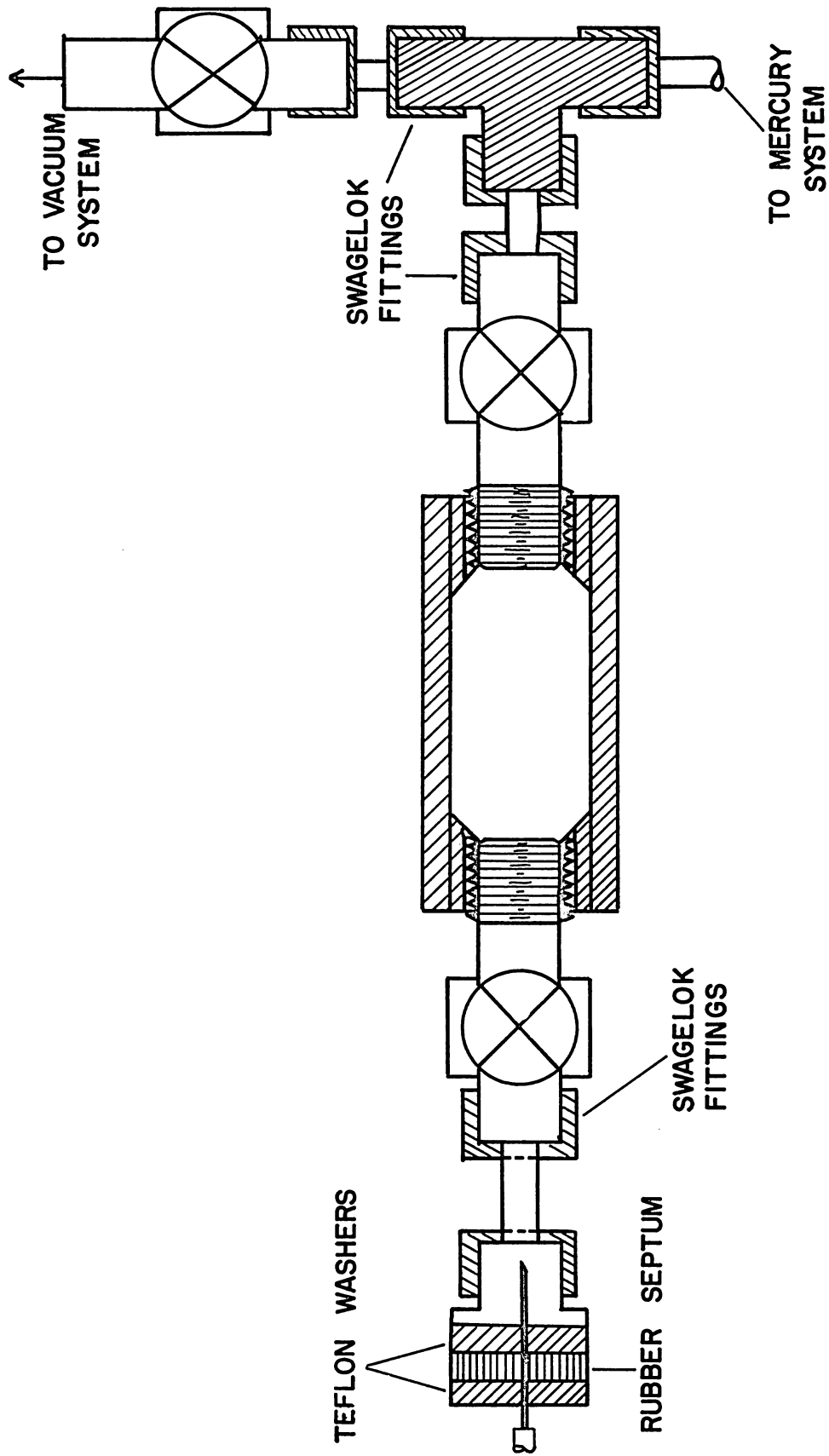
FIG. 4

and New England Nuclear, respectively, came packaged in glass ampoules. These were transferred to more suitable containers which allowed the withdrawal of samples periodically with the syringe as shown in Figures 5 and 6. These containers utilized a mercury reservoir system to maintain the pressure at one atmosphere. The glass containers used for methane and for one sample of ethane were found to be inferior to the stainless steel one used for the other ethane sample. A portion of the tracer samples contained in the glassware escaped over a period of one week or so, primarily due to adsorption in the stopcock grease and in the soft rubber septum. Bulk physical leakage was unlikely due to the absence of any pressure driving force.

The stainless steel container sealed all but a small portion of the ethane between two leak-tight valves. The remaining portion was contained in the sample withdrawal section and was exposed to the rubber septum. This rubber septum was sealed between teflon washers to prevent leakage around the septum. Although the ethane in this small withdrawal section would escape over a period of several weeks, the bulk of the sample could be stored indefinitely.

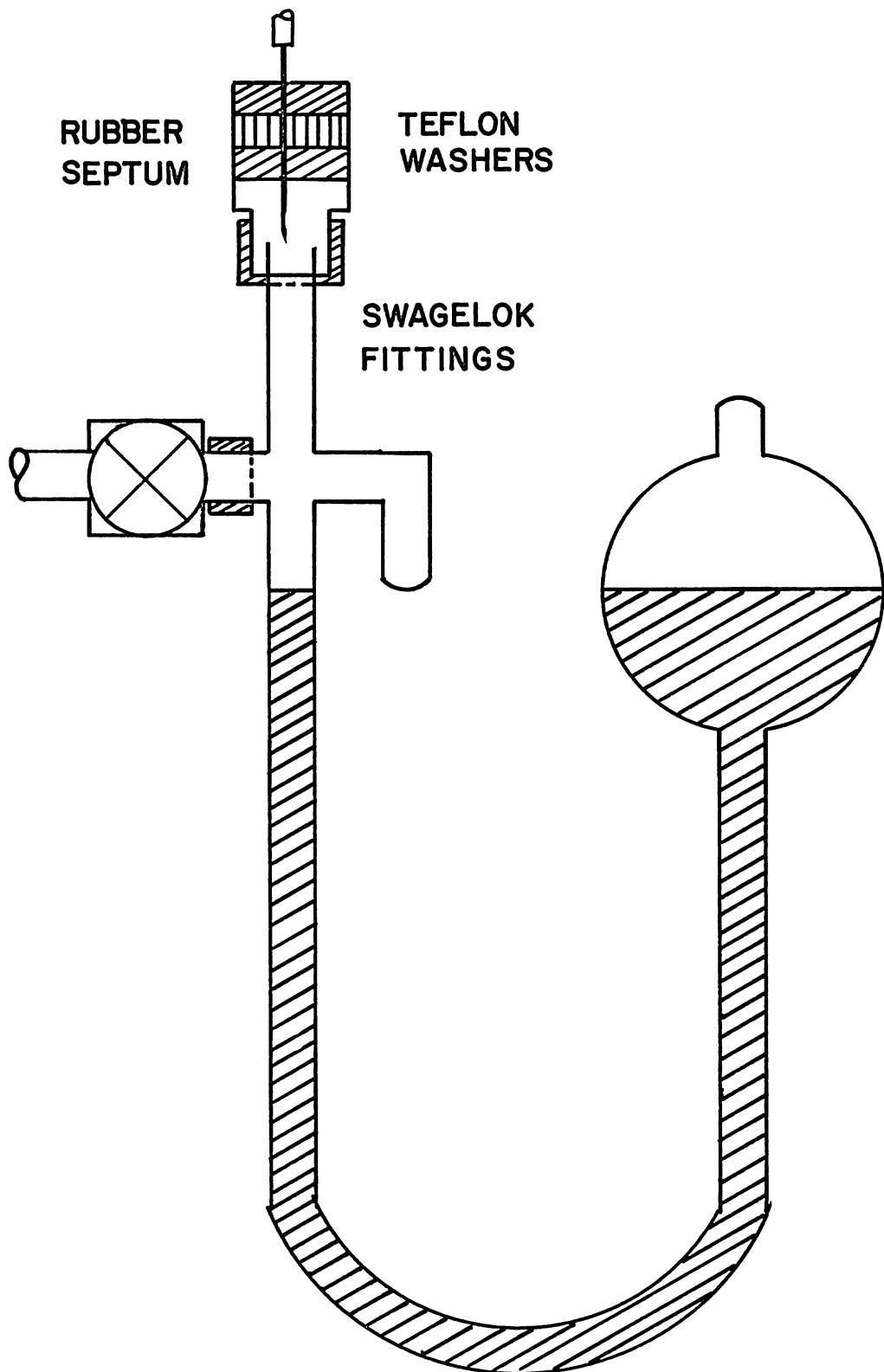
A vacuum system and liquid nitrogen (to freeze the gases into the containers) was used to accomplish the transfer.

The carbon-14 methane and ethane were used full strength as received. The methane had a specific activity of 10.0 mc/mMol, equivalent to 16 mole percent $C^{14}H_4$. The tagged ethane had one C-14 atom per molecule and a specific activity of 5.6 mc/mMol, equivalent to



STAINLESS SAMPLE CONTAINER

FIG. 5



GLASS SAMPLE CONTAINER
FIG. 6

9 mole percent $C^{14}H_3CH_3$. The C-14 decane received from Nuclear-Chicago had a specific activity of 3.0 mc/mMol, which is equivalent to 4.8 mole percent $C^{14}C_9H_{22}$. This was diluted to 0.3 mc/mMol to provide a large enough sample to be injected with the syringe simultaneously with the gaseous tracers.

III. EXPERIMENTAL PROCEDURE

The variables to be measured were the characteristic velocities of the three tracer pulses and the volumetric liquid flow rate.

After setting the bubble flow rate and fillet thickness, the column was allowed to come to steady state. The ratio of bubble volume to fillet volume was determined by the ratio of gas to liquid feed; the bubble frequency was affected by the bubble velocity and to an extent, by the angle of inclination of the bubbler arm. Obtaining the desired frequency and fillet thickness was more art than science, but the bubble velocity was easily controlled with the gas metering valve. The region of high frequency and very thin fillets was somewhat unstable: a sudden jar would collapse the fillets.

All runs were conducted at room temperature. The air conditioning system in the building maintained the temperature at $73.8 \pm 0.7^\circ \text{F}$ so a constant temperature bath was thought not necessary for this work.

Column pressure was maintained constant at slightly above atmospheric pressure by means of the Kendall pressure regulator. System inlet pressure was maintained at a constant pressure of from 0.1 to 0.7 psig.

A small quantity (about .01 to .03 ml) of C-14 methane was first drawn into the syringe, followed by .02 to .04 ml of tagged ethane and .005 ml of decane tracer. The needle was inserted into the sample injection port and the tracers injected. The needle was removed

immediately after injection. The insertion, injection, and removal operations were performed as smoothly as possible to minimize disturbances to the bubbles. Sloppy injection technique often resulted in collapse of the inter-bubble liquid fillets, sometimes throughout the entire column. Needless to say, this caused a huge increase in dispersion, at best, and completely unintelligible results at worse.

At the same time that the sample was injected into the column, a timer was started to record the elapsed time until a reference mark could be placed on the recorder chart.

Soon after injection, collection of a liquid sample was begun and continued until all peaks had exited the column. Sample collection time was recorded and the sample weighed on a Mettler analytical balance. These measurements were used to determine the volumetric liquid flow rate which was in turn used to calculate the liquid to vapor molar ratio in the column.

The helium and the gaseous tracers were vented to the hood which expelled them into the atmosphere. The concentration of tracers in the vented gases was very low (considerably less than one ppm on a volume basis) so that no radioactive hazard was introduced.

The bubble velocity was measured by monitoring the peak retention time of the methane tracer. This retention time had to be corrected for the K value of methane since the methane was partially soluble in the liquid phase. Comparison between measurements based on

the corrected methane retention time and measurements made by timing a bubble over a 100 cm length of tubing showed agreement within $\pm 0.5\%$. It was felt that measurement of the gas velocity with the methane tracer was more accurate than visually timing a bubble, since small variations in the flow rate would still yield an accurate average methane velocity but cause large error in a visual observation made at only one time. Further, it would have been impractical to time a bubble over the entire column length.

The average liquid velocity was measured by recording the C-14 decane peak retention time. It should be mentioned here that some other liquid tracer could have been used to monitor the liquid velocity. All that is required of the liquid tracer is that it be non-volatile and that it form a completely miscible solution with the liquid phase. Carbon-14 decane obviously meets these requirements.

Since ethane is intermediate in volatility between methane and decane, the ethane peak was always observed between the other two peaks.

The count rate meter integration time constant was set for all runs at $\tau = 2$ sec. This was sufficiently small compared to column retention times so that peak distortion was minimal. At $\tau = 0.5$ sec, however, statistical fluctuations were excessive.

The recorder chart speed was varied according to the bubble velocity so that about two to three feet of chart paper was used

per run. This was sufficient for accurate reading of the recorder output peaks.

IV. THEORY

A. Fluid Mechanics Theory

Bretherton² investigated a two-phase system in which a single gas bubble flowed with the liquid phase in a capillary tube. He showed theoretically that the ratio of the liquid film thickness to the tube radius was given by

$$\frac{b}{r} = 0.643 \left(\frac{3\mu V_G}{\sigma} \right)^{2/3} \quad (1)$$

Bretherton tested his theory experimentally and reported good agreement between theory and experiment. Because the liquid film on the wall is stationary, the average linear velocity of the liquid is less than that of the gas bubble. This difference is the basis for the chromatographic effect employed in these measurements.

As Claypool³ has shown, Bretherton's theory can be applied to the bubble column chromatograph system, but with some deviation expected for closely spaced bubbles. He reported excellent qualitative agreement with Bretherton's equation, but quantitative results 5 to 50% lower than predicted. Of greatest significance was the similarity in slopes of $\log(b/r)$ plotted against $\log V_G$.

The relative separation, s , between gas and liquid velocities defined by

$$s = \frac{V_G - V_L}{V_L} \quad (2)$$

was derived by Claypool using the idealized model shown in Figure 7.

His result is

$$s = \frac{1 - \left(1 - \frac{b}{r}\right)^2}{\left(1 - \frac{b}{r}\right)^2} \left(1 + \frac{L_B}{L_L}\right) \quad (3)$$

For small values of b/r , this reduces to

$$s \approx 2 \frac{b}{r} \left(1 + \frac{L_B}{L_L}\right) \quad (4)$$

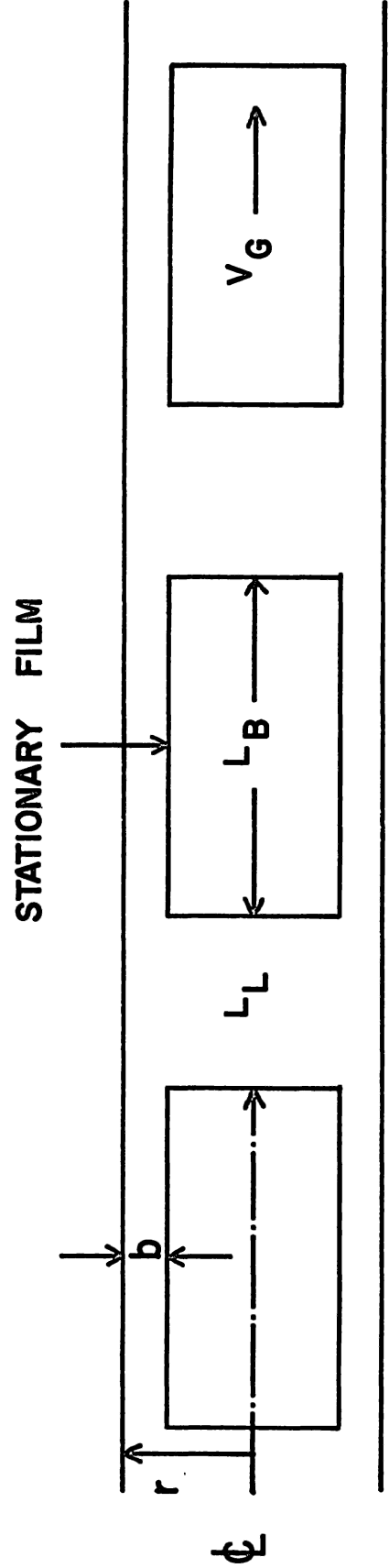
Combined with equation (1), this yields

$$s = 1.286 \left(\frac{3\mu V_G}{\sigma}\right)^{2/3} \left(1 + \frac{L_B}{L_L}\right) \quad (5)$$

Claypool's experimental results for s were lower by about 10% at low velocities (V_G less than 1.2 cm/sec) and appeared to approach a limiting value for a given ratio of L_B/L_L at high bubble velocity.

B. Chromatographic Theory

Deans⁴ has shown that in an ideal chromatographic system, the K value for each component can be obtained from its characteristic velocity; the velocity of the gas and the liquid phases; and the ratio of the moles of liquid to moles of vapor in the column.



IDEALIZED MODEL OF BUBBLE COLUMN

FIG. 7

Making the following assumptions concerning the system:

1. Constant temperature and pressure
2. Infinite dilution of the tracer pulse
3. No diffusion in the longitudinal direction
4. Local equilibrium between phases

one obtains the following partial differential equations describing the mole fractions of component i in each phase

$$C_V \left(\frac{\partial y_i}{\partial t} + V_G \frac{\partial y_i}{\partial z} \right) + R_i = 0 \quad \text{Gas Phase} \quad (6)$$

$$C_L \left(\frac{\partial x_i}{\partial t} + V_L \frac{\partial x_i}{\partial z} \right) - R_i = 0 \quad \text{Liquid Phase} \quad (7)$$

Using the equilibrium relation $y_i = K_i x_i$ or $x_i = \alpha_i y_i$, equations (6) and (7) become

$$C_V \left(\frac{\partial y_i}{\partial t} + V_G \frac{\partial y_i}{\partial z} \right) + R_i = 0 \quad (8)$$

$$\alpha_i C_L \left(\frac{\partial y_i}{\partial t} + V_L \frac{\partial y_i}{\partial z} \right) - R_i = 0 \quad (9)$$

Adding (8) and (9) and rearranging

$$\frac{\alpha_i C_L + C_V}{\alpha_i C_L V_L + C_V V_G} \frac{\partial y_i}{\partial t} = - \frac{\partial y_i}{\partial z} \quad (10)$$

Now using the identity $\left(\frac{\partial t}{\partial z} \right)_{y_i} = - \frac{\partial y_i / \partial z}{\partial y_i / \partial t}$ and

recognizing that $\left(\frac{\partial t}{\partial z}\right)_{y_i} = \frac{1}{V_i}$, when V_i , the characteristic velocity of a pulse of component i , is constant, the following relation is obtained

$$V_i = \frac{\alpha_i \left(\frac{C_L}{C_V}\right) V_L + V_G}{\alpha_i \left(\frac{C_L}{C_V}\right) + 1} \quad (11)$$

Upon rearrangement and insertion of $K_i = 1/\alpha_i$, equation (11) becomes

$$K_i = \frac{C_L V_i - V_L}{C_V V_G - V_i} \quad (12)$$

V. EXPERIMENTAL RESULTS

Table I lists the observed data and the calculated results for the nine runs. Sample calculations for a typical run are given in Appendix A. The gas velocity V_G for run 1 was measured by timing a bubble over a one meter distance at positions of one and nine meters from the beginning of the column. All remaining runs used C-14 methane to tag the gas phase.

The velocities V_1 , V_2 , and V_L (the methane, ethane, and decane velocities respectively) were calculated by dividing column length by respective retention time. The methane velocity was corrected for its finite K value to obtain the true gas velocity V_G . The relative separation, s , defined in the previous section, was calculated from the gas and the liquid velocities.

The liquid to vapor molar ratio in the column was obtained from the volumetric liquid flow rate and the average liquid velocity. The film thickness ratio, b/r , and the bubble length to fillet length ratio were calculated using the idealized bubble column model shown in Figure 7. The normalized peak width \bar{B} was calculated from the decane peak width at half height and the decane retention time. The ethane K value was calculated from the C_L/C_V ratio and the characteristic velocities. Details of the calculational procedure for all the above are contained in Appendix A.

As shown in the Table, the product of the ethane K value and

the average column pressure, K_2P , ranged from 23.63 to 30.49 atm, for an average of 26.60 atm and a mean deviation of 2.10 atm.

Values for the normalized peak width \bar{B} , ranged from .074 to .173 for gas velocities of 1.338 to 3.792 cm/sec in the 1038 cm column, the shorter of the two. Use of the 2278 cm column resulted in less relative dispersion at similar velocities. The longer column had values for \bar{B} of .074 to .114 in the bubble velocity range of 2.199 to 4.068 cm/sec. Figure 8 demonstrates the dependence of \bar{B} on V_G and column length L' .

Values for the dispersion factor $\sqrt{2\sigma_0} \equiv \bar{B} \sqrt{L' V_L}$ ranged from 0.0706 cm/sec^{1/2} to 0.267 cm/sec^{1/2} for bubble velocities of 1.338 to 4.068 cm/sec. Figure 9 demonstrates these results graphically.

The film thickness to tube radius ratio, b/r , varied from .0099 to .0186 as gas velocity increased from 1.338 to 4.068 cm/sec. This is shown graphically in Figure 10.

TABLE 1
DATA AND CALCULATED RESULTS

Run	L' cm	V _G	V ₁ cm/sec	V ₂	V _L	s	b/r	L _B /L _L	P atm.	T °F	\bar{B}	K ₂ P atm
1	1038	2.819	*	2.508	1.989	.417	.0150	12.49	1.034	73.8	.115	23.63
2	2278	4.068	3.957	3.506	2.493	.632	.0186	15.49	1.038	73.2	.114	23.65
3	1038	3.792	3.695	3.288	2.044	.855	.0175	22.80	1.013	73.2	.173	24.99
4	1038	1.832	1.800	1.665	1.069	.714	.0123	27.57	1.024	73.8	.120	27.49
5	1038	3.144	3.070	2.796	1.997	.574	.0160	16.44	1.026	73.8	.128	27.34
6	1038	2.232	2.190	2.052	1.661	.344	.0128	12.21	1.028	74.1	.096	29.71
7	1038	1.338	1.319	1.247	0.9096	.471	.0099	22.42	1.022	74.1	.074	30.49
8	2278	2.727	2.671	2.438	1.331	1.049	.0140	35.76	1.035	74.1	.089	27.40
9	2278	2.199	2.157	1.957	1.024	1.147	.0131	41.86	1.033	74.5	.074	24.67

*For run 1, the gas velocity was measured by timing a bubble over a measured distance of one meter.

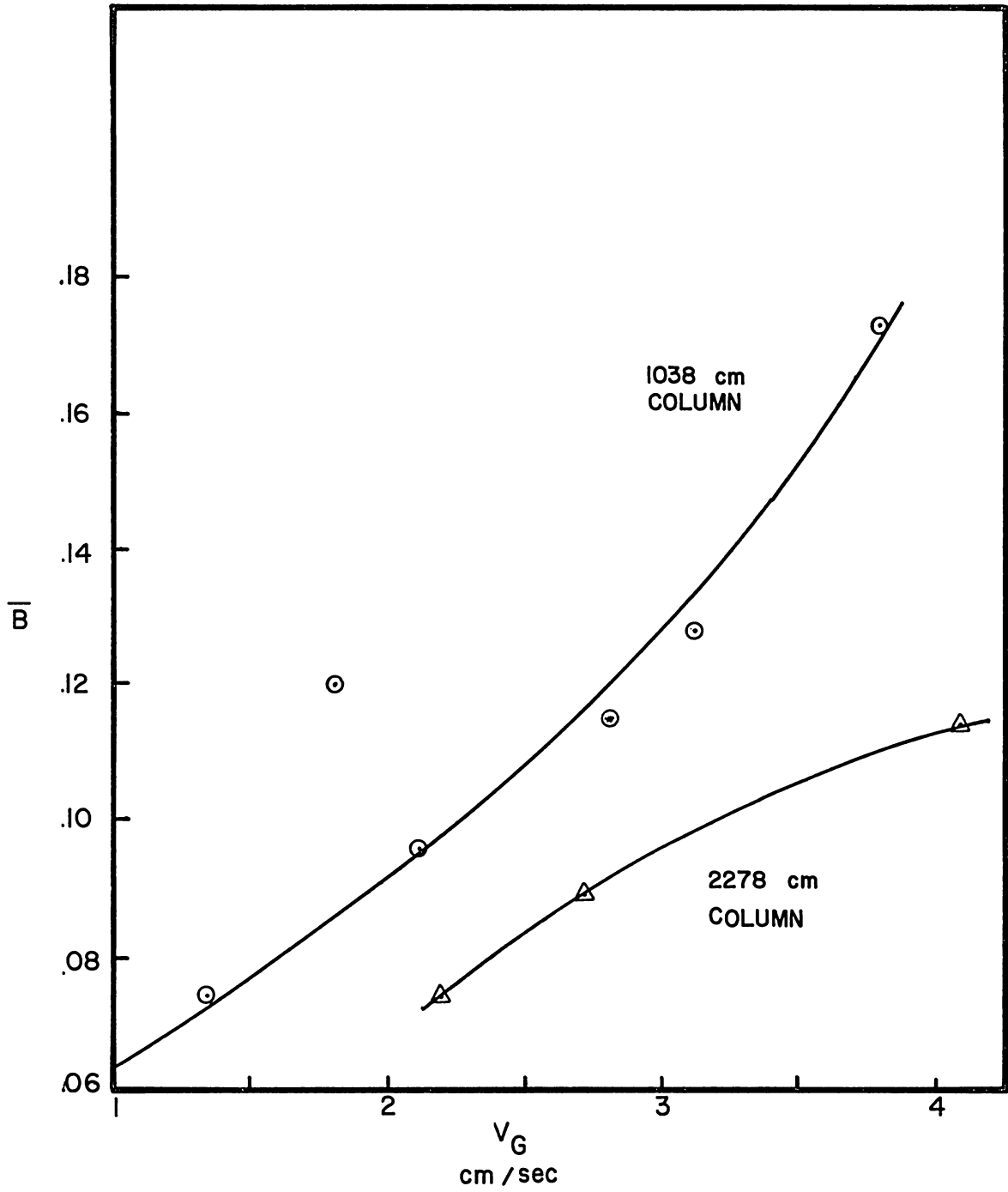


FIG. 8 NORMALIZED PEAK WIDTH VS. GAS VELOCITY

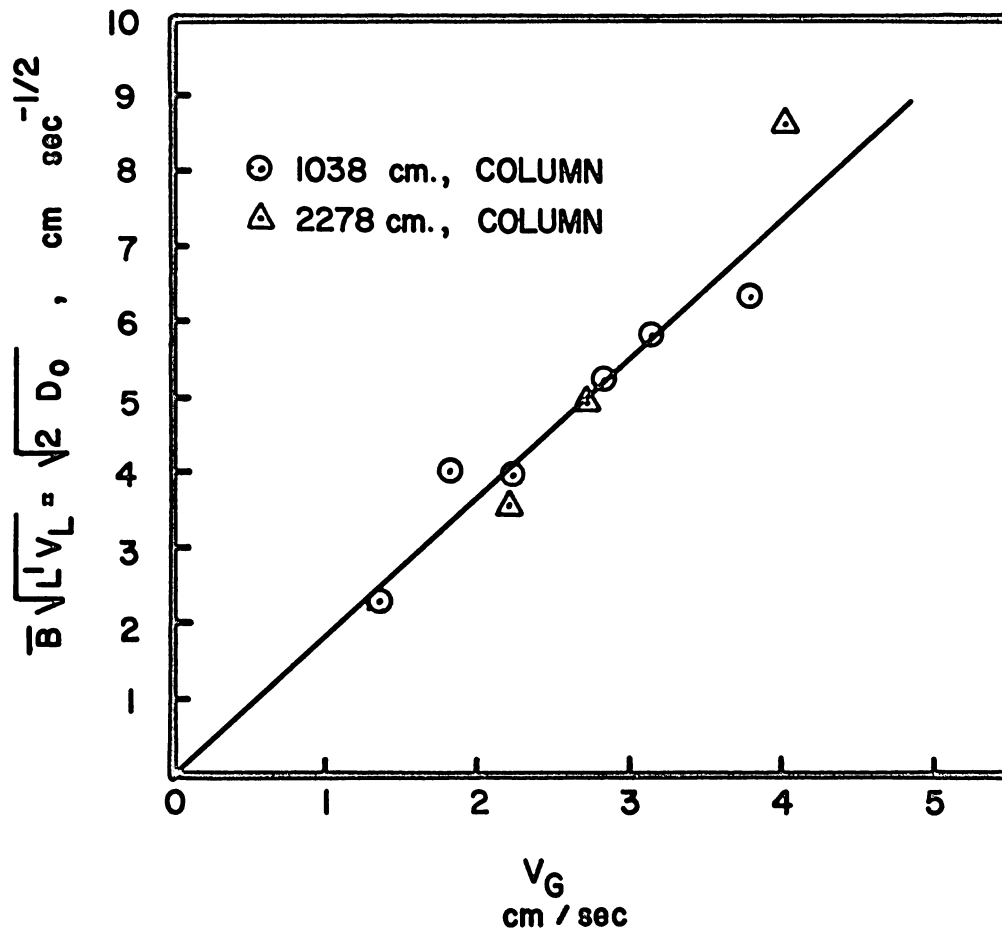


FIG. 9 OVERALL DISPERSION COEFFICIENT
 VS. GAS VELOCITY

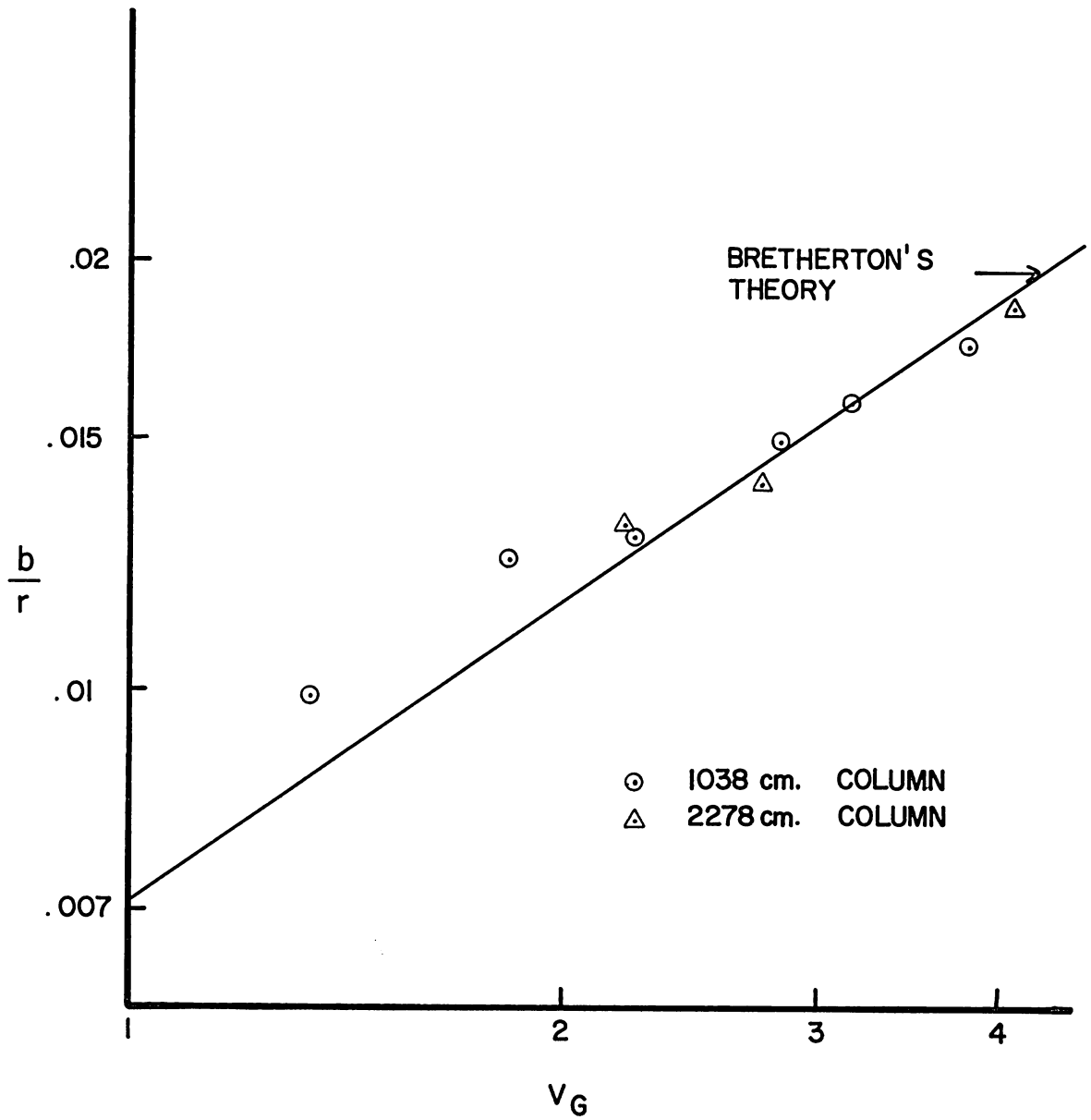


FIG. 10 FILM THICKNESS VS. GAS VELOCITY

VI. DISCUSSION OF RESULTS

K Value Data:

Table 1 reports the ethane K values as the product of the column pressure and the K value. This in effect normalizes the K values to the same condition of one standard atmosphere pressure. This approach is valid since the product K_1P is very nearly constant over small pressure ranges far from the critical point.

The K_2P value obtained with the bubble column ranged from 23.63 to 30.49 for an average of 26.60 and a mean deviation of 2.10. This compares favorably with 25.5 from the NGPSA⁸ for ethane at one atmosphere and interpolated to 74 °F. Stalkup and Kobayashi¹² reported 27.8 at 70 °F which extrapolated gives 28.7 at 74 °F. The results of this work lie within experimental deviation of the preceding two references.

The nine runs were obtained at room temperatures of 73.8 ± 0.7 °F. Such small differences in temperature have very little effect on the K value of ethane. The NGPSA⁸ data shows that K_2 varies by only 0.28 per degree F in the neighborhood of 74 °F.

Dispersion:

Figure 8 shows the normalized peak widths \bar{B} as a function of bubble velocity with column length as a parameter. The figure shows that dispersion or peak spreading increases with V_G and decreases with

column length.

The overall dispersion coefficient \mathcal{D}_o is defined by

$$\mathcal{D}_o \equiv \frac{(B^*)^2}{2t} \quad (1)$$

where B^* is the peak width in cm. Now since $B^* = \bar{B} L'$ and $t = L'/V_L$, \mathcal{D}_o can be equivalently defined by

$$\mathcal{D}_o \equiv \frac{\bar{B}^2 L' V_L}{2} \quad (2)$$

$$\bar{B} \sqrt{L' V_L} = \sqrt{2\mathcal{D}_o} \quad (3)$$

Figure 9 demonstrates the dependence of $\sqrt{2\mathcal{D}_o} \equiv \bar{B} \sqrt{L' V_L}$ on the gas velocity V_G . The graph shows a linear relationship between $\sqrt{2\mathcal{D}_o}$ and V_G . This result is equivalent to Claypool's³ theory which related \mathcal{D}_o to velocity squared and to his results which indicated that the dispersion coefficient was proportional to the 1.9 power of V_G .

No attempt was made to measure or correlate the gas phase dispersion in a quantitative manner. It was observed, however, that the methane peak width was always less than a fifth of the decane peak, and further that the ethane peak was generally a little wider than the peak from the more volatile methane. These qualitative observations are in accord with what one would expect. Since the bubbles are discrete, direct mass transfer from bubble to bubble is impossible and gas phase dispersion should be confined to individual bubbles. What

gas phase dispersion was noticed was most likely due to tracer injection technique since the tracer was initially distributed over several bubbles. The tracer samples were not sufficiently concentrated to allow injection into one bubble alone. The ethane peak dispersion was greater than the methane because more of the ethane was present in the more dispersive liquid phase.

Film Thickness:

Bretherton's² theory predicted that the film thickness was related to the gas velocity by

$$\frac{b}{r} = .643 \left(\frac{3\mu}{\sigma} \right)^{2/3} (V_G)^{2/3}$$

Values for b/r were obtained from this equation using values of 23.5 dynes/cm for the surface tension and .907 cps for the viscosity of decane, both at 74 °F¹³. The agreement between theory and experiment as shown in Figure 10 is quite good except in the low velocity region. The theory would be expected to break down at low V_G since it erroneously predicts zero film thickness at zero velocity. Claypool's observation that b/r approaches a limiting value at high velocity could neither be confirmed nor denied by this work.

VII. CONCLUSIONS AND PROJECTION OF TECHNIQUE

The conclusion of this work is that the determination of vapor-liquid equilibria by horizontal bubble chromatography is indeed feasible and is certainly worthy of further study.

Extension of this method to higher temperatures and pressures is limited only by the physical properties of the liquid phase, the most important of which is the surface tension. Bubble formation depends vitally upon this parameter which, by definition, vanishes at the critical point. Obviously then, the bubble column chromatograph cannot be used to study equilibria near the critical. How close is "close" remains to be determined, however.

At moderate pressures, the effect of pressure on the surface tension is small. Hirschfelder, Curtiss, and Bird⁵ report that surface tension is directly proportional to the fourth power of the difference between the liquid and vapor densities. For gas densities of ten percent of the liquid density (requiring fairly high pressures) the surface tension will still be 66 percent of that in vacuum.

Higher temperatures also decrease surface tension. From 0 °F to 200 °F, the surface tension of n-decane in vacuum decreases from 27.7 to 17.3 dynes/cm. Thus, both higher temperatures and pressures will decrease this important parameter.

The experimental work covered in this thesis used an insoluble carrier gas ($K = \infty$) and a non-volatile liquid phase ($K = 0$)

since this is the simplest case. Extension to a general multicomponent system with no restrictions on the K values introduces some complications. (The details are discussed in Appendix C.)

Now that bubble chromatography has been shown to be feasible, it should now be possible to refine the technique for better accuracy and to extend it to systems of n components of unrestricted equilibrium properties.

APPENDIX A
Calculations

1. Procedure

The K value was previously shown to be dependent on the characteristic velocities and the liquid to vapor molar ratio:

$$K_i = \frac{C_L}{C_V} \frac{V_i - V_L}{V_G - V_i} \quad (1)$$

Consider again the simplified bubble column shown in Figure 7. Let v_G and v_L denote the volume of gas and of liquid respectively in a unit bubble. Their molar ratio will be given by

$$\frac{C_L}{C_V} = \frac{v_L}{v_G} \frac{zRT}{P} \frac{\rho_L}{M_L} \quad (2)$$

Now the total liquid volume v_L is composed of the fillet moving at velocity V_G and the stationary film along the wall and is related to the velocities by

$$v_L V_L = (v_L)_{\text{wall}} (0) + (v_L)_{\text{fillet}} V_G \quad (3)$$

$$v_L = (v_L)_{\text{fillet}} \frac{V_G}{V_L} \quad (4)$$

Now the fillet volume is related to the gas volume by

$$(v_L)_{\text{fillet}} = (v_G) \frac{L_L}{L_B} \quad (5)$$

so by combining (2), (4), and (5), one gets

$$\frac{C_L}{C_V} = \frac{L_L}{L_B} \frac{V_G}{V_L} \frac{zRT}{P} \frac{\rho_L}{M_L} \quad (6)$$

The length of a fillet L_L is given by

$$L_L = \frac{Q}{\theta F \rho_L A_T (1 - b/r)^2} \quad (7)$$

and the bubble length L_B by

$$L_B + L_L = \frac{V_G}{F} \quad (8)$$

Combining (7) and (8)

$$\frac{L_B}{L_L} = \frac{V_G \rho_L A_T (1 - b/r)^2 \theta}{Q} - 1 \quad (9)$$

Since V_L/V_G is the fraction of all liquid that is in the moving fillet

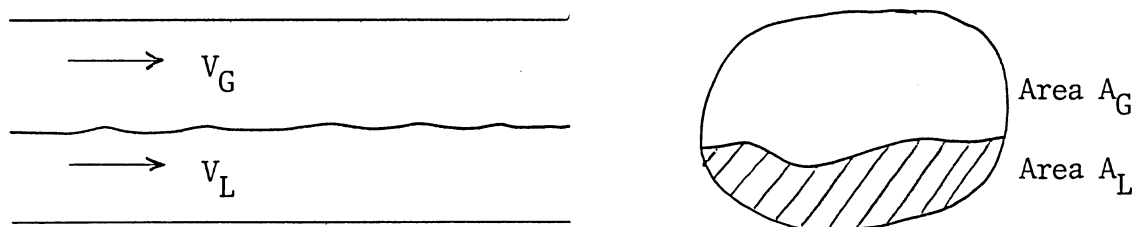
$$\frac{V_L}{V_G} = \frac{(1 - b/r)^2}{\frac{L_B}{L_L} (1 - (1 - b/r)^2) + 1} \quad (10)$$

Upon rearranging equation (10)

$$(1 - b/r)^2 = \frac{V_L \left(\frac{L_B}{L_L} + 1 \right)}{V_L \left(\frac{L_B}{L_L} \right) + V_G} \quad (11)$$

While the above development has assumed an ideal bubble model for computing C_L/C_V , there is no dependence of the result on the assumption. The idealized model has simply permitted the calculation of idealized parameters which are of interest (L_B/L_L and b/r) but which are unnecessary for obtaining C_L/C_V and the K values.

To demonstrate the independence of C_L/C_V from the model, consider the following general chromatograph model with cross-sectional areas of flow of A_G and A_L for the gas and liquid respectively.



The volumetric liquid flow rate, F_L , is given by

$$F_L = \frac{Q}{\theta \rho_L} = A_L V_L \quad (12)$$

The total area of flow, A_T , is known, so that

$$A_G = A_T - A_L \quad (13)$$

The ratio of the gas area to liquid area is

$$\frac{A_G}{A_L} = \frac{A_T - \frac{F_L}{V_L}}{\frac{F_L}{V_L}} = \frac{A_T V_L \theta \rho_L}{Q} - 1 \quad (14)$$

This ratio of A_G to A_L is the same as the volume ratios, so combining with equation (2) results in the following expression for the liquid to vapor ratio:

$$\frac{C_L}{C_V} = \frac{Q}{A_T V_L \theta \rho_L} - Q \frac{zRT}{P} \frac{\rho_L}{M_L} \quad (15)$$

Equation (15) does in fact produce results identical to those obtained by simultaneous iterative solution of equations (6), (9), and (11).

Measurement of the gas velocity with tagged methane produces a V_1 which is not the true gas velocity since methane has a finite K value and its retention time is increased by solution in the liquid phase. Thus, correction must be made for the discrepancy. The methane tracer also obeys equation (1):

$$K_1 = \frac{C_L}{C_V} \frac{V_1 - V_L}{V_G - V_1} \quad (16)$$

Solving for V_G , the true gas velocity

$$V_G = V_1 + \frac{C_L}{C_V} \frac{V_1 - V_L}{K_1} \quad (17)$$

This equation is then solved after solving for C_L/C_V and the results plugged into equation (1)

$$K_2 = \frac{C_L}{C_V} \frac{V_2 - V_L}{V_G - V_2} \quad (18)$$

2. Sample Calculation

The following data was obtain for run 2:

V_1	3.957 cm/sec
V_2	3.506
V_L	2.493
Q	1.5930 g
θ	319.3 sec
P_{av}	1.0375 atm
T	73.2°F
A_T	.0288 cm ² (all runs)
ρ_L	.729 g/cm ³
M_L	142.3 g/mol

Plugging into equation (15) for C_L/C_V

$$\frac{C_L}{C_V} = \frac{1.5930}{(.0288)(2.493)(319.3)(.729) - 1.593} \frac{(1.)82.06}{1.8} \frac{532.92}{1.0375} \frac{.729}{142.3}$$

$$\frac{C_L}{C_V} = 12.65$$

Now correcting for the methane K value

$$V_G = 3.957 + 12.65 \frac{3.957 - 2.493}{166.7} = 4.068$$

and

$$K_2 = 12.65 \frac{3.506 - 2.493}{4.068 - 3.506}$$

$$= 22.80$$

$$K_2P = 23.65$$

APPENDIX B

Discussion of Isotope Effects

The work covered by this thesis used carbon-14 tracers for peak detection in the procedure for obtaining the ethane K value. Since what was actually accomplished was the calculation of the K value of carbon-14 ethane, it is important that the normal and radioactive isomers have very similar vapor-liquid equilibrium properties.

Bigeleisen¹ applied quantum theory to the isotope effect on physical and thermodynamic properties including vapor pressure and showed that simple correlations based only on the ratio of molecular weights were unsatisfactory since equivalent isomers could be shown to have different properties.

Van Hook¹⁴ studied the vapor pressures of normal ethane compared to 1, 1-C₂H₄D₂ which has the same molecular weight as C-14 ethane. At 200 °K, he reported that the deuterated ethane had a 2.1% higher vapor pressure. Extrapolated to 300 °K (using other data below 200 °K as a guide), the difference is only 1.2%.

Van Hook and Kelly¹⁵ used gas chromatography to determine the ratio of K values of the deuterated isomers of ethane. At 273 °K, he found that the C₂H₄D₂ isomers had K values about 2% greater than the normal ethane.

Koonce⁷ determined the infinite dilution K values of propane and carbon-14 propane by gas-liquid chromatography. At 70 °F he

could detect no reproducible difference, reporting differences of -0.4 and -0.8%, which were less than the average error of reproducibility. Over a wide range of 125 data points, he reported an average deviation of less than one percent.

Kobayashi⁶ has determined that the ratio of the K values of methane and singly deuterated methane is on the order of 1.0002.

While it is not completely established that the K values of the carbon-14 isomers are within 2% or less of each other, it seems highly probable that they are, based on the previous evidence. Furthermore, the average experimental deviation of 9% is higher than the possible 2% or so isotope effect, so that any isotope effect would have been undetectable in this experiment.

APPENDIX C

Extension of Technique

Extension to a binary system with no restrictions on the K values introduces some minor complications. The liquid density which is needed to calculate C_L/C_V will depend on composition. The average liquid molecular weight will also change. The z parameter in the equation of state for the vapor will depend on composition as well as on temperature and pressure. Furthermore, an equilibrium flash calculation will be required. For a binary system, this will be a direct, non-iterative procedure. The descriptive relations will be

$$y_n = \frac{K_n (K_o - 1)}{K_o - K_n} \qquad y_o = 1 - y_n$$

$$x_n = \frac{y_n}{K_n} \qquad x_o = y_o / K_o$$

$$\rho_L = \rho_L(x_o)$$

$$z = z(y_n)$$

$$M_A = x_o M_o + x_n M_n$$

$$\frac{C_L}{C_V} + \frac{Q}{A_T V_L \theta \rho_L - Q} = \frac{zRT}{P} \frac{\rho_L}{M_A}$$

For the particular case of a non-volatile liquid, the preceding equations reduce to

$$y_0 = 1 \qquad y_n = 0$$

$$x_0 = 1/K_0 \qquad x_n = 1 - 1/K_0$$

$$z = \text{constant} \qquad \rho = \rho(x_0)$$

$$M_A = \frac{M_0}{K_0} + \frac{M_n}{1 - 1/K_0}$$

For the general case of n components with no restrictions on their K values, an iterative solution of $4n + 3$ simultaneous equations will be required. The steady-state feed and column exit overall compositions and molar flow rates will of course be the same. Also, the exit mole fractions x_i and y_i will be the same as the internal column mole fractions, although the ratio of liquid to vapor molar flow rate will not be the same as C_L/C_V . Therefore, the overall compositions inside the column and in the feed respectively will not be the same. The overall feed composition will presumably be known, so one arrives at the following equations describing the system:

$$x_i \frac{C_L}{C_V} + y_i = z_i \frac{C_L}{C_V} + 1$$

$$x_i \frac{L}{V} + y_i = z_i^* \frac{L}{V} + 1$$

$$x_i = y_i/K_i$$

$$\frac{L}{V} = \frac{C_L}{C_V} \frac{V_L}{V_G}$$

$$K_i = \frac{C_L}{C_V} \frac{V_i - V_L}{V_G - V_i}$$

$$M_A = \sum x_i M_i$$

$$\frac{C_L}{C_V} = \frac{Q}{A_T V_L \theta \rho_L - Q} \frac{zRT}{P} \frac{\rho_L}{M_A}$$

There are $4n + 3$ unknowns and the same number of equations and the K values of all n components can be determined simultaneously.

It is interesting to notice the effect of the limiting case in which the liquid phase is stationary. The set of equations is now insoluble because C_L/C_V is indeterminate. This is the situation for standard gas-liquid chromatography unless an additional non-volatile component is added to the liquid phase. The fundamental reason for the investigation of bubble chromatography is the desire to avoid the added component.

APPENDIX D
Original Data

TABLE II

Run	Retention Times, sec			Collected	Collection
	t_1	t_2	t_L	Liquid, g Q	Time, sec θ
1	368.2	413.8	521.8	1.4349	337.2
2	575.7	649.7	913.7	1.5930	319.3
3	280.7	315.7	507.7	2.1046	651.6
4	577.0	624.0	971.0	0.7883	600.0
5	338.1	371.3	519.7	1.4050	383.4
6	473.9	505.9	624.9	2.0088	581.1
7	787.2	832.2	1141.2	1.3831	1176.3
8	852.8	934.4	1711.6	2.9193	1928.5
9	1056.0	1164.0	2224.0	1.5057	1435.7

BIBLIOGRAPHY

1. Bigeleisen, Jacob, J.Chem.Phys. 34, 1485 (1961)
2. Bretherton, F.P., J.Fluid Mechanics 10, 166 (1961).
3. Claypool, D.D., M. S. thesis, Rice University, Houston, Texas, 1967.
4. Deans, H.A. Private communication (1968).
5. Hirschfelder, J.O., Curtiss, C.F., and Bird, R.B., Molecular Theory of Gases and Liquids. John Wiley & Sons, Inc., New York, 1954.
6. Kobayashi, Riki. Private communication (1968).
7. Koonce, K.T., Ph.D. thesis, Rice University, 1963.
8. Natural Gas Processors Suppliers Association, Engineering Data Book, Tulsa, Okla. (1966).
9. Owen, G.R., M. S. thesis, Rice University, Houston, Texas 1965.
10. Ramin, R.E., M.S. thesis, Rice University, Houston, Texas, 1966.
11. Reamer, H.H. and B.H. Sage, J.Chem.Eng.Data 7, 161 (1962).
12. Stalkup, F.I. and Riki Kobayashi, A.I.Ch.E. Journal 9, 121 (1963)
13. Technical Data Book - Petroleum Refining. American Petroleum Institute, New York, 1966.
14. Van Hook, W. Alexander, J.Chem.Phys. 44, 237 (1966).
15. Van Hook, W. Alexander and Margaret E. Kelly, Anal. Chem. 37, 508 (1965).